

# Supporting Information

## Improving the Design of Nanoparticle pH Sensors for Intracellular Measurements

### Authors:

Rikke V. Benjaminsen<sup>1</sup>, Honghao Sun<sup>1</sup>, Jonas R. Henriksen<sup>1</sup>, Nynne M. Christensen<sup>1</sup>, Kristoffer Almdal<sup>1</sup> and Thomas L. Andresen<sup>1,\*</sup>

<sup>1</sup>Technical University of Denmark, DTU Nanotech, Department of Micro- and Nanotechnology, Frederiksborgvej 399, 4000 Roskilde, Denmark

\*Corresponding author: Tel: +45 45258168; E-mail: [thomas.andresen@nanotech.dtu.dk](mailto:thomas.andresen@nanotech.dtu.dk)

## Synthetic procedure of nanosensor preparation

**Dual-labeled sensor.** Was synthesized as described previously (Sun et al., J. Biomed. Nanotechnol. 5, 676–682, 2009).

**Tripple-labeled sensor.** The nanosensor synthesis has been carried out on various scales. Typically, 2.04 g of acrylamide, 0.51 g of methylbisacrylamide, and 0.052 g of (3-propylamine) methylacrylamine hydrochloride were dissolved in 6.15 mL of milliQ water. 5.7 mL of this monomer solution was added drop wise to 240 mL of oil phase, which was prepared by dissolving 62.5 g TX-100 and 153.27 g 1-hexanol in 1000 ml cyclohexane. A reverse microemulsion was formed under stirring for 10 min, after which the reaction mixture was degassed through four freeze-vacuum-thaw cycles and kept under argon atmosphere. 60uL of 25% (w/w) ammonium persulfate solution and 40uL of tetramethylethylenediamine were added to initiate the polymerization. The reaction was stirred at room temperature for 3 h, and the reaction mixture was monitored by  $^1\text{H}$  NMR to ensure full conversion. The nanosensors were precipitated by addition of ethanol, and then filtered using an Amicon ultra-filtration cell (Millipore Corp., Bedford, MA). The NPs was redispersed in MilliQ water with ultrasonic treatment and was dialyzed against MilliQ water. A solution of fluorescein isothiocyanate, Oregon Green isothiocyanate and rhodamine B isothiocyanate were added to 1mL NP-NH<sub>2</sub> aqueous solution (50 mg/mL), after which the pH was adjusted to 8 using PBS buffer. The reaction mixture was stirred for 4 hours and dialyzed against MilliQ water to remove free fluorophore.

## Methods for calculating pH as a function of R.

The inverted function of equation (1), for the measurement of pH with a dual-labeled nanosensor:

$$pH = pKa - \log \left( \frac{R_s + R_o - R}{R - R_o} \right) \quad (\text{S1})$$

For the triple-labeled nanosensor, the pH can be calculated by solving this quadratic equation, obtained from equation (2):

$$10^{pKa_1+pKa_2} \cdot x^2 + \left(10^{pKa_1} + 10^{pKa_2} - \frac{R_1}{R - R_0} \cdot 10^{pKa_2} - \frac{R_2}{R - R_0} \cdot 10^{pKa_1}\right) \cdot x + 1 - \frac{R_1 + R_2}{R - R_0} = 0$$

Where  $x = 10^{-pH}$  (S2)

### Derivation of a generalized form of equations (1) and (2).

The pH experienced by the sensor is accessed by measuring fluorescence intensities from co-localized pH responsive probes and a pH independent reference probe. As the composition of the sensor particle is fixed, the influence of the sensor concentration on the pH measurement is removed by ratiometric analysis, where the fluorescence intensity of the pH responsive probes is normalized with respect to the fluorescence intensity of the reference probe. This fluorescence ratio is expressed as:

$$R = (\Phi_{pH} - \Phi_{pH}^B) / (\Phi_R - \Phi_R^B)$$

where  $\Phi_{pH}$ ,  $\Phi_{pH}^B$  and  $\Phi_R$ ,  $\Phi_R^B$  are the acquired fluorescence intensities and corresponding background of the pH-sensitive probes and reference probe respectively. We have derived a generalized relation:

$$R = \sum_{i=1}^n \frac{R_i}{(1+10^{pKa_i-pH})} + R_0 \quad (S3)$$

relating the fluorescence ratio,  $R$  and pH for a sensor incorporating  $n$  pH responsive and one reference probe. Equation (S3) is based on the assumptions: (i) no interference between the fluorophores of the sensor, (ii) linear response of the fluorescence intensity with respect to the fluorophore and sensor concentration and (iii) protonation of the  $i$ 'th fluorophore ( $F_i$ ) is described by the equilibrium:  $HF_i \rightleftharpoons F_i^- + H^+$ , which is governed by  $10^{-pKa_i} = [F_i^-][H^+] / [HF_i]$ . In equation (S3),  $pKa_i$  defines the protonation state of the  $i$ 'th fluorophore,  $R_i$  relates to the change in quantum yield of the  $i$ 'th fluorophore upon de-protonation and  $R_0$  is the fluorescence ratio of the fully protonated sensor.

### Determination of background levels.

For the determination of background levels all pixels in one color channel in an image were presented in a histogram in relation to their intensity values. In these images most pixels are background and indeed the main peak situates at low intensities, with the rest of the pixels spread out evenly over the rest of the intensity interval up to 255. Figure S1 shows the histogram of low intensities and the corresponding cumulative distribution function of the red channel from an image of HepG2 cells with internalized triple-labeled nanosensor. The background level, determined collectively for all images in an experiment, was determined as the intensity at the middle of the steep part of the cumulative distribution function, here 4.2. This value was then subtracted as background for all images of the experiment, including corresponding calibration images. The green channel was corrected the same way.

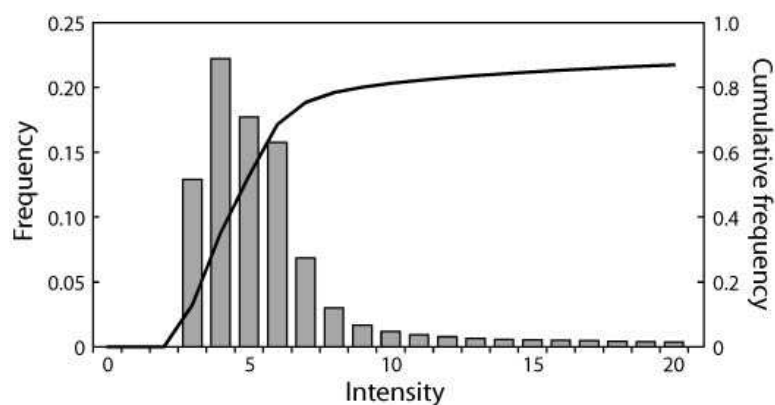


**Figure S1. Histogram and cumulative distribution function of background level.** From an image of HepG2 cells with internalized triple-labeled nanosensor, all pixels in the red channel were plotted in a histogram according to their intensity, and the corresponding cumulative distribution function. The image is zoomed in on the low intensities as the rest, up to 255, shows a long relatively flat tail.

### Comparison of image processing by two different methods.

The experiment presented in Figure 2a top and 2b of HepG2 cells with internalized triple-labeled nanosensor before and after treatment with bafilomycin A<sub>1</sub> was analyzed by the two different image analysis methods; Either based on Region Of Interests (ROIs) of nanosensor containing vesicles or by a

pixel by pixel analysis as described in Methods. The pH histograms obtained by the two methods are presented in Figure S2. The two methods show identical histograms with comparable mean and standard deviation.

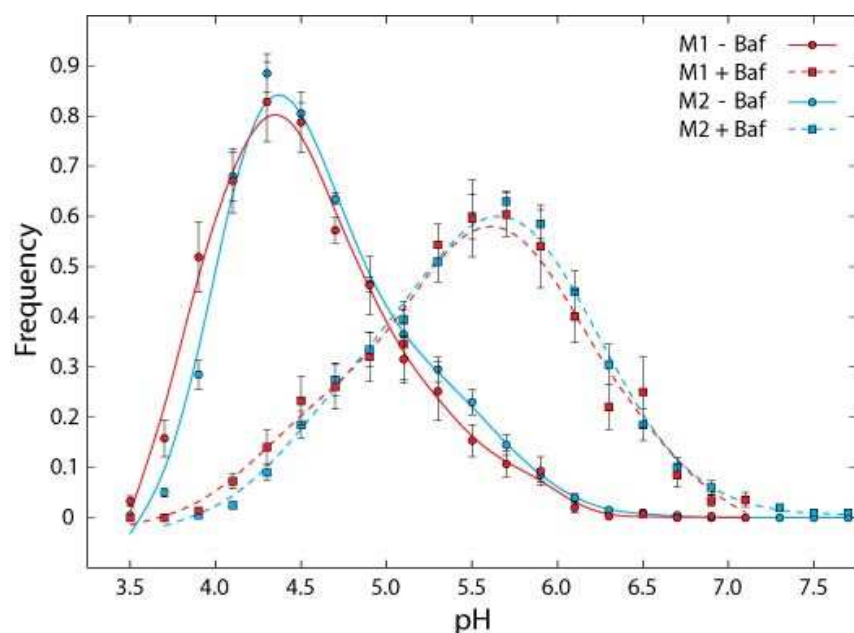


**Figure S2. Comparison of histograms obtained with two different image analysis methods.** HepG2 cells with internalized triple-labeled nanosensor were imaged before and after treatment with bafilomycin A<sub>1</sub> for 30 min. Images were analyzed by two methods and the resulting histograms presented with mean  $\pm$  SEM (n = 9 and 8 cells before and after treatment respectively).

### **Temporal pH measurements following bafilomycin A<sub>1</sub> treatment.**

HepG2 cells were treated with the new triple-labeled nanosensor for 24 h, washed three times with ice cold PBS supplemented with heparin, once with PBS and kept in growth medium without phenol red for analysis by confocal microscopy. Cells were imaged before treatment with 50 nM bafilomycin A<sub>1</sub>, and the same cells were then imaged every five min after the addition of bafilomycin A<sub>1</sub>. The change in average pH of all vesicles in a cell is shown in Figure S3. Every cell was imaged seven times, and in order to exclude that the effect was caused by differential photobleaching of the fluorophores and not bafilomycin A<sub>1</sub>, control experiments were performed. Cells with internalized nanosensor were imaged

continuously for more than seven images without any further treatment. This experiment showed no or only very small fluctuations in pH between the seven images showing that it is the treatment with bafilomycin A<sub>1</sub> that is causing the increase in pH. The same result was obtained when performed on cells after treatment with bafilomycin A<sub>1</sub> for 30 min.

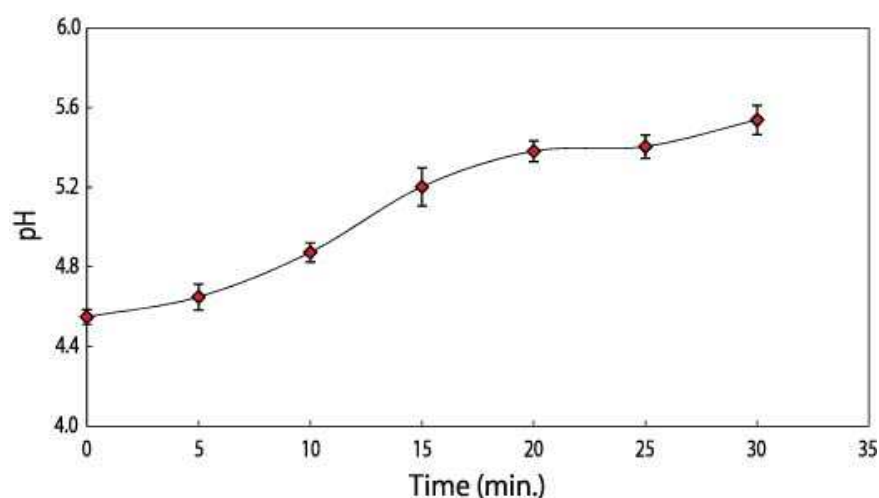


**Figure S3. Temporal measurements following bafilomycin A<sub>1</sub> treatment.** Nanosensor containing cells were treated with bafilomycin A<sub>1</sub>, and imaged every five min. pH was calculated for every nanosensor containing vesicle and the average within an entire cell was calculated. Presented are mean ± SEM (n ≥ 7 cells). Representative of six independent experiments.

### Colocalization of neutral nanoparticle with lysosomes and endosomes.

A colocalization experiment was performed between a neutral RhB-labeled nanoparticle (-0.1 mV and 80 nm) and the GFP-tagged markers GFP-LAMP-1 for lysosomes and GFP-Rab5a for endosomes. Colocalization images can be seen in Figure S4. Experiment was performed identically to the experiment with a positive particle in the main article. This particle also showed significant colocalization with GFP-LAMP-1, with an overlap coefficient of 62 % and a Pearson's correlation coefficient of 0.61, whereas colocalization with the early endosomal marker Rab5a nor showed colocalization with coefficients of 20 % and 0.14 respectively.

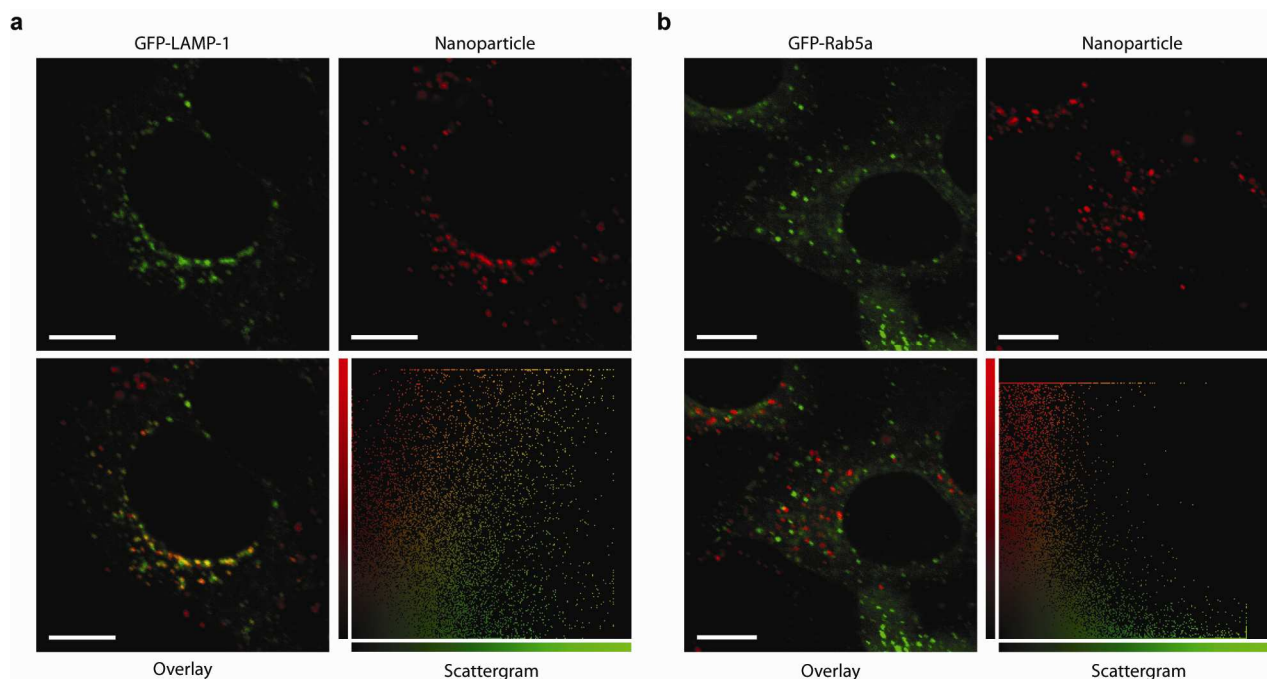


**Figure S4. Colocalization of neutral nanoparticle with lysosomes and endosomes.** Colocalization of a neutral RhB-labeled nanoparticle with **a**, lysosomal marker GFP-LAMP-1 and **b**, early endosomal marker GFP-Rab5a. HepG2 cells were transduced with plasmids encoding GFP tagged marker and incubated with nanoparticle for 24 h. Top left image: GFP tagged lysosomal/endosomal marker, top right: nanoparticle, bottom left: overlay and bottom right: Scattergram of all pixels in overlay relating green intensity to red intensity of the same pixel. Scale bar, 10  $\mu\text{m}$ . Representative of three independent experiments.

### Cytotoxicity of nanosensor.

HepG2 cells were seeded in 96 well plates with 4000 cells per well and allowed to adhere for 24 h, cells were then treated with increasing concentrations of nanosensors for 24 h. The XTT assay were performed according to manufacturer's instructions (In Vitro Toxicology Assay Kit, XTT based (TOX-2), Sigma-Aldrich). Briefly, nanosensor containing media were aspirated from cells and fresh media containing 200  $\mu\text{g}/\text{ml}$  XTT was added and the plate was incubated in the dark over night. Absorbance was measured with an ELISA reader (VICTOR<sup>3</sup> 1420 Multilable Counter, PerkinElmer Life Science Wallac Denmark A/S) at 450 nm. Viability of the cells in response to a neutral (39 nm and 4.3 mV) and a positively charged

(113 nm and 23.9 mV) dual-labeled (FS-RhB) nanosensor is presented in Figure S5. Appropriate controls were included in order to exclude absorbance and other artifacts caused by nanosensors. Positively charged nanoparticles show a significantly higher cytotoxicity than neutral particles with an  $IC_{50}$  value of  $\sim 35 \mu\text{g/ml}$  versus  $IC_{50} \geq 1000 \mu\text{g/ml}$  for the neutral particle. The pH measurements were done with a slightly positive particle (4.6 mV) at the concentration  $10 \mu\text{g/ml}$ , where the particles do not show any significant cytotoxicity.

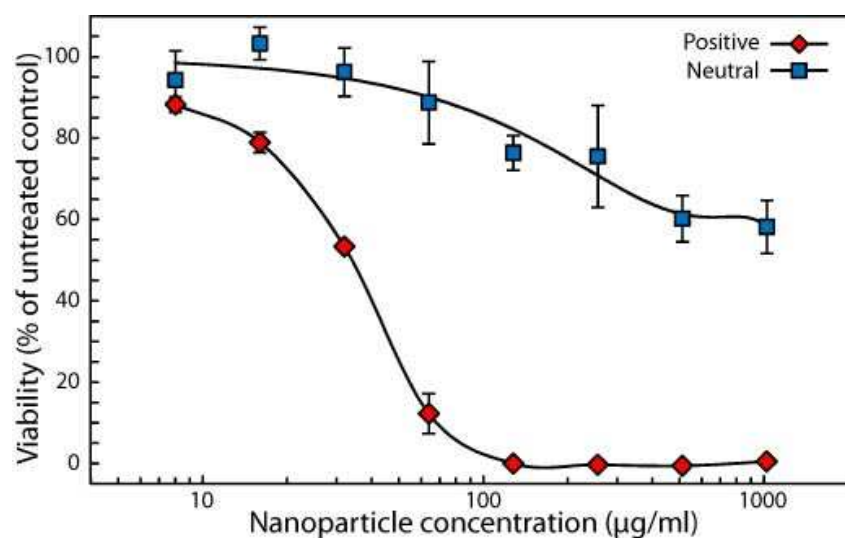


**Figure S5. Cytotoxicity of the nanosensor.** HepG2 cells were treated with different concentrations of a positive and a neutral nanoparticle, and the viability of the cells was analyzed with the XTT assay. Results are presented as the mean  $\pm$  SD of triplicate wells in relation to untreated control cells. Representative of three independent experiments.

#### Calibration of the triple-labeled nanosensor in buffer.

Calibration of the triple-labeled nanosensor was done in buffer on different days, and with different microscope settings, e.g. laser power and gain. All calibration curves were fitted to equation (2) for a triple-labeled sensor, and then normalized (by subtraction of  $R_{\min}$  and division by  $(R_{\max} - R_{\min})$ ). Five different normalized calibration curves can be seen in Figure S6. It is evident that these curves are very



similar and shows the same pKa values. Therefore, we reason that calibration can be done by measuring the intensity ratios of the triple-labeled nanosensor at only two pH values for every experiment. Having these ratios, a normalized calibration curve can be converted to fit experimental data acquired on different days and with different microscope settings.

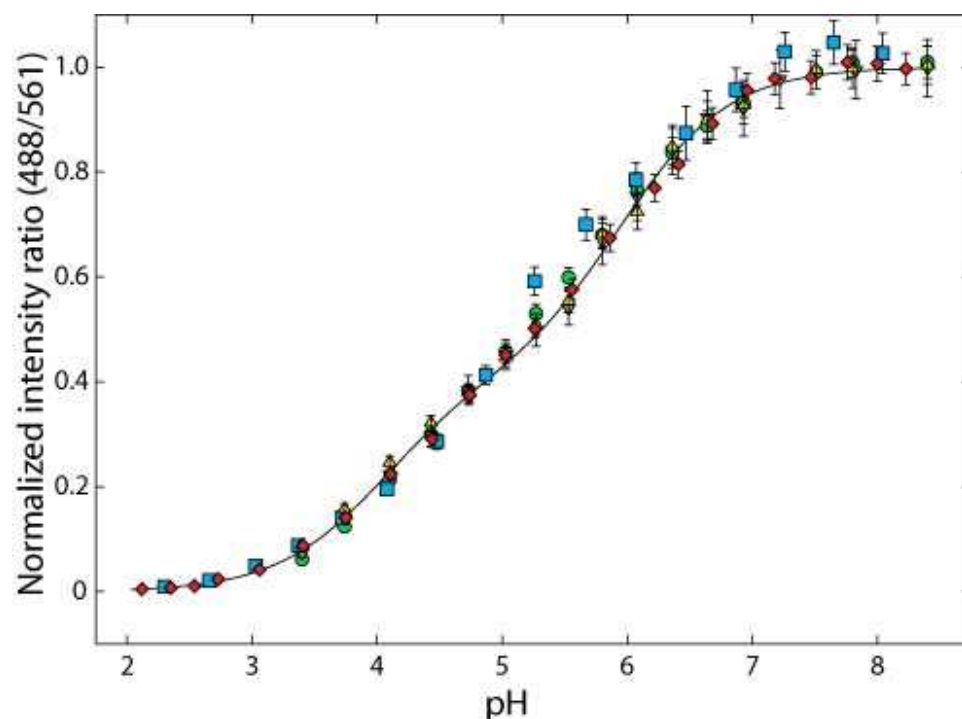


**Figure S6. Calibration of triple-labeled nanosensor.** Calibration of the triple-labeled nanosensor was performed in buffer on different days and with different microscope settings. Five different calibration curves are presented with the normalized intensity ratio as a function of pH. Mean  $\pm$  SD of 450 ROIs within each image are presented.